

1    **Strong divergent selection at multiple loci in two closely related species of ragworts adapted**  
2    **to high and low elevations on Mount Etna**

3

4    Running title: Strong selection in ragworts on Mount Etna

5

6    Edgar L.Y. Wong<sup>1,\*</sup>, Bruno Nevado<sup>1</sup>, Owen G. Osborne<sup>1,3</sup>, Alexander S.T. Papadopoulos<sup>1,3</sup>, Jon R.  
7    Bridle<sup>2</sup>, Simon J. Hiscock<sup>1</sup> and Dmitry A. Filatov<sup>1</sup>

8

9    <sup>1</sup>Department of Plant Sciences, University of Oxford, Oxford, OX1 3RB, UK

10    <sup>2</sup>School of Biological Sciences, University of Bristol, Bristol, BS8 1UG, UK

11    <sup>3</sup>Current Address: Molecular Ecology and Fisheries Genetics Laboratory, Environment Centre

12    Wales, School of Natural Sciences, Bangor University, Bangor, LL57 2UW, UK

13

14    \*corresponding author: Edgar L.Y. Wong, [edgar.wong@plants.ox.ac.uk](mailto:edgar.wong@plants.ox.ac.uk)

15    **Abstract**

16    Recently diverged species present particularly informative systems for studying speciation and  
17    maintenance of genetic divergence in the face of gene flow. We investigated speciation in two  
18    closely related *Senecio* species, *S. aethnensis* and *S. chrysanthemifolius*, which grow at high  
19    and low elevations, respectively, on Mount Etna, Sicily and form a hybrid zone at intermediate  
20    elevations. We used a newly generated genome-wide single nucleotide polymorphism (SNP)  
21    dataset from 192 individuals collected over 18 localities along an elevational gradient to  
22    reconstruct the likely history of speciation, identify highly differentiated SNPs, and estimate  
23    the strength of divergent selection. We found that speciation in this system involved  
24    heterogeneous and bidirectional gene flow along the genome, and species experienced  
25    marked population size changes in the past. Furthermore, we identified highly-differentiated  
26    SNPs between the species, some of which are located in genes potentially involved in  
27    ecological differences between species (such as photosynthesis and UV response). We  
28    analysed the shape of these SNPs' allele frequency clines along the elevational gradient. These  
29    clines show significantly variable coincidence and concordance, indicative of the presence of  
30    multifarious selective forces. Selection against hybrids is estimated to be very strong (0.16 –  
31    0.78) and one of the highest reported in literature. The combination of strong cumulative  
32    selection across the genome and previously identified intrinsic incompatibilities likely work  
33    together to maintain the genetic and phenotypic differentiation between these species –  
34    pointing to the importance of considering both intrinsic and extrinsic factors when studying  
35    divergence and speciation.

36    **Keywords**

37    speciation, gene flow, selection, adaptation, hybrid zone

## 38 **Introduction**

39 Defining what constitutes a species and understanding how new species form are central  
40 questions in evolutionary biology. The idea that speciation is driven by adaptation to distinct  
41 environmental conditions has a long history going back to Darwin's concept of new species  
42 formation by means of natural selection. Although natural selection is the main driver of  
43 evolutionary changes, its role in creating barriers to gene flow is not well understood.  
44 Adaptation to distinct environments (divergent selection) may lead to differentiation in loci  
45 responsible for adaptation or even fixation of different alleles in isolated populations. This can  
46 generate a mosaic with different genomic regions having different extents of gene flow, and  
47 consequently, genetic divergence (Feder, Egan, & Nosil, 2012; Mallet, 2005; Teeter et al., 2008;  
48 Wu, 2001). This effect allows evolutionary biologists to study genetic and phenotypic  
49 differences between species in relation to environmental or ecological change, and in areas  
50 where populations meet, such as hybrid zones. Hybrid zones, and more generally systems in  
51 which reproductive isolation is incomplete, are powerful tools for this purpose. This is because  
52 the basis of reproductive isolation and recombinants can be more easily detected in these  
53 systems without being obscured by post-speciation divergence.

54 Genetic and phenotypic trait differences between species or populations can be  
55 tracked along geographical clines. Parameters of clines are informative about the strength of  
56 selection and dispersal rate (Barton & Gale, 1993; Barton & Hewitt, 1985; Szymura & Barton,  
57 1986; 1991), while cline coincidence and concordance inform us about selective pressures in  
58 the hybrid zone. For instance, both coincidence and concordance could suggest they are  
59 influenced by their respective gradients (whether identical or different) in a similar way  
60 (Barton & Gale, 1993; Kruuk et al., 1999; Young, 1996); whereas discordant clines could

61 suggest the presence of several external selective pressures (Durrett, Buttel, & Harrison, 2000).  
62 Tracking the change in allele frequency or trait values along the clines allow us to evaluate the  
63 nature, magnitude and relative importance of selection in shaping the hybrid zone, thus  
64 enable a deeper understanding of microevolutionary bases of local adaptation and  
65 reproductive isolation. Several studies have estimated the strength of selection in different  
66 systems (Table 1), with estimated selection coefficient ranging from as low as 0.0017 to over  
67 0.7. Surprisingly, although interspecific hybridisation is common in plants, there is a lack of  
68 selection estimates for plant hybrid zones [e.g. Antonovics & Bradshaw, 1970 (this study  
69 estimated selection using a different method compared to the one in our study); Brennan et  
70 al., 2009]. Our study aims to fill this gap, providing a detailed analysis of selection maintaining  
71 an altitudinal hybrid zone in *Senecio* on Mount Etna, Sicily.

72         It is thought that the chance of local adaptation leading to speciation can be increased  
73 by either strong selection on a single trait or selection on a larger number of traits (stronger  
74 selection and multifarious selection hypotheses; Nosil, Harmon, & Seehausen, 2009).  
75 Although speciation with one or few traits have been well characterised, an increasing number  
76 of cases are reporting the presence of multifarious selection in different systems. For example,  
77 selection by both breeding pool acidity and predators in frogs (*Rana arvalis*; Egea-Serrano,  
78 Hangartner, Laurila, & Räsänen, 2014), selection on female oviposition preference and  
79 diapause initiation in butterflies (*Lycaeides* sp.; Gompert et al., 2013), selection on various  
80 diapause life-history traits in flies (*Rhagoletis* sp.; Daroski & Feder, 2007), and selection on  
81 floral colour and other ecophysiological traits in monkeyflowers (*Mimulus aurantiacus*; Sobel  
82 et al., 2019; Stankowski et al., 2017). In cases where there is multifarious selection, although  
83 selection on each trait might not be strong enough to cause speciation on its own, it is the

84 cumulative effect of many selective agents that leads to strong reproductive isolation and  
85 divergence overall; genetic hitchhiking leading to correlated response of many genes could  
86 also be effective in driving divergence in the multifarious selection scenario (Nosil et al., 2009).

87 In this study, we created clines for several genetic and phenotypic markers, and  
88 estimated the strength of selection against hybrids in an altitudinal hybrid zone in two *Senecio*  
89 (Asteraceae) species on Mount Etna, Sicily. We also reconstructed the history of their  
90 speciation and describe the interplay among demography, gene flow and selection in this  
91 system. The two study species, *Senecio aethnensis* and *Senecio chrysanthemifolius*, maintain  
92 a hybrid zone at their intermediate elevations at around 1,000 – 2,000m (Chapman, Forbes, &  
93 Abbott, 2005; James & Abbott, 2005), where they exhibit a range of intermediate phenotypes  
94 between the two species (Brennan, Bridle, Wang, Hiscock, & Abbott, 2009; James & Abbott,  
95 2005). *S. aethnensis* and *S. chrysanthemifolius* habitats show contrasting environmental  
96 conditions, both elevation- and ecology-related, such as temperature, solar radiation, and  
97 water availability (James & Abbott, 2005; Körner, 2007; Ross, 2010). Their divergence was  
98 estimated to have occurred less than 200,000 years ago, coinciding with the rise of Mount  
99 Etna to elevations above 2,000 m due to volcanic activity (Chapman, Hiscock, & Filatov, 2013;  
100 Muir, Osborne, Sarasa, Hiscock, & Filatov, 2013; Osborne, Batstone, Hiscock, & Filatov, 2013).  
101 Typical *S. aethnensis* occurs above 2000 m whereas typical *S. chrysanthemifolius* occurs below  
102 1000 m (Brennan et al., 2009; Muir et al., 2013). Both species are short-lived, obligately  
103 outcrossing perennials pollinated by generalist insects and bear wind-dispersed fruits; they  
104 can be distinguished by several morphological and physiological characters, such as degree of  
105 leaf dissection, size of capitula and florets, and flowering time (Brennan et al., 2009; James &  
106 Abbott, 2005). The two species produce fertile hybrids (Chapman et al., 2005), but significant

hybrid breakdown in F<sub>2</sub> hybrids (Chapman, Hiscock, & Filatov, 2016), and evidence of genetic incompatibilities (Brennan, Hiscock, & Abbott, 2014; 2016; 2019; Chapman et al., 2016) suggests the two are distinct species that have evolved substantial reproductive isolation.

Previous demographic studies in this system (Filatov, Osborne, & Papadopoulos, 2016; Chapman et al., 2013; Muir et al., 2013; Osborne et al., 2013) have shown the presence of low on-going gene flow between the species. It was also demonstrated that an allopatric phase during divergence of the two *Senecio* species is unlikely (Filatov et al., 2016). Other studies have identified differentially expressed genes (Chapman et al., 2013); investigated geographic clines in the Etnean *Senecio* system using phenotypic data, allozymes and simple sequence repeats, and estimated moderate selection against hybrids (0.02 - 0.41; Brennan et al., 2009); and mapped hybrid breakdown to several quantitative trait loci (Chapman et al., 2016). However, these studies have not directly tested for other demographic parameters (such as heterogeneous gene flow and population size change), patterns of gene flow within the hybrid zone, and the extent of divergent selection. In our study, we addressed these issues specifically using finer scale sampling throughout the geographical cline on the southern side of Mount Etna, combined with analysis of leaf morphology and genetic diversity based on reduced-representation genomic data (“nextRAD”; Russello, Waterhouse, Etter, & Johnson, 2015). We hypothesize that: 1) as reproductive isolation is incomplete, the two species would show demographic features of recent speciation with gene flow, such as heterogeneous gene flow; 2) the system is under multifarious selection thus there would be many genetic markers under various strengths of divergent selection; and 3) there is strong cumulative selection against hybrids to maintain species divergence despite on-going gene flow. To test these hypotheses, we: 1) reconstructed the likely speciation scenario in this system, specifically

including hybrid groups and demographic models comprising parameters previously unexplored; 2) identified potential genomic targets of divergent selection and carried out cline analysis on them; and 3) estimated the strength of selection in the hybrid zone. These analyses allowed us to infer the patterns of gene flow in different parts of the hybrid zone and the extent of selection that is responsible for the maintenance of species identity and build-up of species divergence despite on-going interspecific gene flow.

## **Materials and Methods**

### **Sampling**

To infer the extent of genome-wide divergence between *S. aethnensis* and *S. chrysanthemifolius*, and the potential selective pressures acting on this system, we generated and analysed data comprising reduced-representation nextRAD sequences (Russello et al., 2015) and leaf dissection measurements. The same individuals were used in generating both datasets. A total of 192 individuals from 18 localities were sampled over an elevational gradient from 585 m to 2,645 m on a transect on the southern side of Mount Etna. These include six typical *S. aethnensis* (above 2,000 m) localities, three typical *S. chrysanthemifolius* (below 1,000 m) localities and nine hybrid localities (Fig. 1d); nine to 14 individuals were sampled from each locality (Table S1). Leaf material was collected and dried in silica gel for DNA extractions; while fresh leaves were collected from each individual on site and photographed on top of gridded paper for measurements.

### **nextRAD sequencing**

In the nextRAD dataset, the two highest and lowest elevation localities were previously used in a demographic study (Filatov et al., 2016), while the remaining 14 localities are new additions to the dataset. Genomic DNA was extracted from dried leaves using a modified CTAB protocol (Doyle & Doyle, 1987) and purified with QIAGEN DNeasy mini-spin columns. DNA was then sent to SNPsaurus (Oregon, USA), who prepared nextRAD sequencing libraries and carried out 150b single-end Illumina sequencing. This approach is similar to RAD-seq, but uses degenerate primers instead of restriction enzymes.

#### **Analyses of raw reads, genetic diversity and structure in nextRAD dataset**

Raw reads from nextRAD sequencing were processed using *STACKS v1.34* (Catchen, Amores, Hohenlohe, Cresko, & Postlethwait, 2011). The *process\_radtags* function was used to remove any reads that contained uncalled bases and other low-quality reads. The *denovo\_map.pl* script was then used to create a *de novo* catalogue of loci and genotype reads. A minimum stack depth (option -m) of 15, maximum number of mismatches between loci of the same individual (option -M) of two, and maximum number of mismatches between loci in the catalogue (option -n) of two were allowed in making the *de novo* catalogue. The *populations* function was used to call SNPs from the samples, calculate genetic diversity statistics (number of private alleles, percentage of polymorphic loci, observed heterozygosity, expected heterozygosity, nucleotide diversity, inbreeding coefficient, and pairwise  $F_{ST}$ ), and create genotype input files for further analyses using other software packages. SNPs with 50% or less missing data were retained for subsequent analyses. Isolation by distance was assessed using pairwise genetic distance [ $F_{ST}/(1-F_{ST})$ ] and difference in elevation or geographic distance between locality pairs, with Mantel test, all carried out in *IBD v1.52* (Bohonak, 2002). Analysis



of molecular variance (AMOVA), using only localities involved in demographic modelling, was carried out to test that polymorphism is mostly within species or hybrid groups instead of among individual localities (see demographic modelling section below for details on grouping). To assess the genetic clustering within the dataset, we carried out a principal component analysis (PCA) with the R package *ade4* (Bougeard, 2018; Chessel, Dufour, & Thioulouse, 2004; Dray, Dufour, & Chessel, 2007; Dray & Dufour, 2007) and *factoextra* (Alboukadel & Fabian, 2017). Missing data in PCA were replaced with mean allele frequencies. We also used *STRUCTURE* (Pritchard, Stephens, & Donnelly, 2000) to analyse the clustering of samples. In this analysis, the admixture model was used and the data was run for  $K = 2$  to 18, with 10 iterations for each  $K$ . 200,000 generations of burn-in was performed, with 100,000 generations retained. The value for  $K$  was then determined using the ad hoc statistic  $\Delta K$  (Evanno, Regnaut, & Goudet, 2005) calculated with *Structure Harvester v0.6.94* (Earl & vonHoldt, 2012).

#### **Demographic modelling using nextRAD data**

To explore the demographic history of the two *Senecio* species and their hybrids and visualise the two-dimensional site frequency spectra (2D-SFS), we investigated 14 demographic models (Fig. S2) using Poisson random field-based demography inference framework implemented in the *dadi* package (Gutenkunst, Hernandez, Williamson, & Bustamante, 2009). For this analysis, localities were pooled to represent each of the typical species localities and hybrid localities at the top and bottom of the hybrid zone (inferred from *STRUCTURE* plot): localities 1 to 3 (585 – 910 m) were pooled to represent typical *S. chrysanthemifolius* (C); localities 7 to 9 (1,310 – 1,515 m) were pooled to represent low-elevation hybrids (LH); localities 12 to 14

198 (1,880 – 2,090 m) were pooled to represent high-elevation hybrids (HH); localities 16 to 18  
 199 (2,386 – 2,645 m) were pooled to represent typical *S. aethnensis* (A). This pooling strategy was  
 200 necessary to increase the number of samples in each group. To avoid artificially inflating gene  
 201 flow between groups through pooling localities, AMOVA was carried out to test that  
 202 polymorphism is mostly within these groupings instead of among individual localities.  
 203 Moreover, a test run using only one locality of each typical species (locality 1 and 18) were  
 204 consistent with those from pooled localities. Since no outgroup data was available, folded site  
 205 frequency spectra (SFS) were generated for each group using the python script easySFS.py  
 206 (accessed from <https://github.com/isaacovercast/easySFS>). Following recommendations in  
 207 the *dadi* manual, each group's sample size was projected down to 10 to 14 alleles (i.e. SNPs  
 208 with less than these numbers of alleles scored will be removed, and those with more were  
 209 subsampled to these numbers) to deal with missing data across individuals. SFS of the species  
 210 pair was first analysed under 14 models of isolation with migration and secondary contact (Fig.  
 211 S2), which were published previously (Tine et al., 2014; Filatov et al., 2016; Nevado, Contreras-  
 212 Ortiz, Hughes, & Filatov, 2018) or modified from them. These models vary in complexity (see  
 213 detailed flow chart in Fig. S2), with the simplest one (*split*) having no population size change  
 214 and no migration between populations since splitting; to more complex models that allow  
 215 migration rate in one direction only (e.g. *IM1*, *IM2*), same migration rate for both directions  
 216 (e.g. *split\_mig*, *IM2M\_1*), different migration rates in each direction (e.g. *SC*, *IM*, *IMpre*),  
 217 different migration rates at different times (e.g. *SplitExpMig*, *eSplitExpMig*) or at different  
 218 parts of genome (e.g. *IM2M*) and population size fluctuations (e.g. *eSplitExpMig*, *IM*, *IMpre*,  
 219 *IM2M*). Several models are used in this study to test conditions that were not explored before,  
 220 such as unidirectional gene flow (*IM1*, *IM2*), heterogeneous gene flow (*IM2M*), and a

secondary contact scenario with population size change (*eSC*, *SC\_IM2M*). Since the models *IM2M* (heterogeneous gene flow since divergence) and *SC\_IM2M* (period of no gene flow followed by heterogeneous gene flow after secondary contact) both have high likelihoods, a more complex model comprising features of both, *IM2M\_AL\_SC*, was included. This model assumes speciation with heterogeneous gene flow, followed by a period of no gene flow, then secondary contact with heterogeneous gene flow. For all models, 10 runs were performed initially for each data group using a wide parameter range (0 – 5 for time parameters, 0 – 10 for migration parameters, 0 – 100 for size parameters). A further set of 30 runs were then performed using narrower parameter ranges around the optimal values identified in the initial runs.

Since not all the models are nested, the best-fitting model was selected based on Akaike Information Criterion (AIC). The best-fitting model was chosen based on the lowest AIC score. Robustness of parameter estimates of the two best-fitting models was evaluated with 100 bootstrap runs, with the confidence intervals calculated as  $M \pm 1.96X$  (where  $M$  is the likelihood parameter estimate and  $X$  is the standard deviation from Godambe Information Matrix (GIM) across replicates). Likelihood ratio tests were performed for nested models to assess which features of models were important in the demographic history of *Senecio* on Mount Etna (refer to Fig. S2 for visualization of models). In particular, *split\_mig* and *split* were used to test whether migration has been important; *IM* and *IM1* or *IM2* were used to test whether migration in only one direction would better fit the data; *IM* and *IMpre* were used to test whether there was population size change before the split. *IM2M\_1* and *IM2M* were used to test whether having two classes of migration rates provided significantly better fit.

After ranking the demographic models for the pair of pure species, the best model (*IM2M*) and another simpler isolation with migration model (*IM*) were fitted to data from five other comparisons involving pure species and hybrids: high- and low-elevation hybrids (HH/LH), *S. chrysanthemifolius* and low-elevation hybrids (C/LH), *S. chrysanthemifolius* and high-elevation hybrids (C/HH), *S. aethnensis* and low-elevation hybrids (A/LH) and *S. aethnensis* and high-elevation hybrids (A/HH). This is to determine finer scale demographic patterns between species and hybrid localities at different elevations and to compare gene flow in each direction over various spatial separation. These two models have the same type of migration parameters (heterogeneous gene flow or two unidirectional migration) as *SC\_IM2M* (the other highly likely model) and *eSC*; they are run since they have fewer parameters than the latter two while yielding the same type of migration data.

#### **Measurement of leaf phenotype**

Leaf dissection is the most morphologically distinct character between *S. aethnensis* and *S. chrysanthemifolius*, which have undissected and highly dissected leaves respectively. Hybrids show gradual changes in leaf dissection along the elevation gradient, suggesting that this trait is under divergent selection. To quantify the differences in leaf dissection between the typical species and their hybrids, leaf area to perimeter ratio was used as a proxy for degree of dissection (same trait used in Brennan et al., 2009; 2016). Leaf area to perimeter ratio was calculated from leaf photographs taken at the time of collection. Four to 10 fresh leaves from each individual were collected to control for within individual variability in leaf size. They were photographed on top of gridded paper for measurements. Leaf areas and perimeters were measured using the software ImageJ (Schneider, Rasband, & Eliceiri, 2012). Leaf area to

perimeter ratio was then calculated for each leaf and averaged across leaves for each individual.

#### **Identification of outlier loci in the nextRAD dataset**

Fixation index  $F_{ST}$  was calculated for each SNP across all samples using *Arlequin* (Excoffier, Laval, & Schneider, 2005), and P values were adjusted for false discovery rate (Benjamini–Hochberg procedure). Negative  $F_{ST}$  was treated as zero. Another Bayesian-based outlier scan was carried out using *BayeScan* (Foll & Gaggiotti, 2008) to estimate the probability of a SNP being under selection. This analysis was carried out using default settings: 20 pilots runs of 5,000 iterations, followed by 50,000 burn-in iterations and 5,000 iterations using a thinning interval of 10. Prior odds was set to 10,000. SNPs were treated as outliers if they were significant in both analyses – markers with adjusted P value smaller than 0.05 in *Arlequin* and  $\log_{10}PO$  larger than 1 (which indicates selection is 10 times more likely than neutral differentiation at the SNP) in *BayeScan*.

To test if the SNPs are part of or in proximity to any functional genes, a blast search of the loci containing the outlier SNPs was first carried out against genomic scaffolds of *S. squalidus* (unpublished; *S. squalidus* is the hybrid species between *S. aethnensis* and *S. chrysanthemifolius* that originated *ex situ* in the UK). Only non-duplicated matches with at least 95% base pair and 90% identity matched were retained. Sequences within 10 kb from the markers were then blasted against the non-redundant protein sequences database of NCBI. Gene Ontology (GO) terms of top blast hit genes were identified using UniProt (<https://www.uniprot.org/>).

## Cline fitting

Maximum likelihood fitting of clines was done to leaf dissection means or mean allele frequency along the elevational gradient for the leaf area to perimeter ratio, and each of the 76 outlier markers. Elevation is used instead of geographic distance because 1) genetic distance has a stronger correlation with difference in elevation than geographic distance (Fig. 3); 2) environmental or ecological selective pressures likely change with elevation but not geographic distance; and 3) it allows direct comparison of cline centre and widths at particular elevations in different studies in the system, whereas use of geographic distance would cause confusion as different transects might start and end at different locations. Cline fitting was carried out using the R package *HZAR* (Derryberry, Derryberry, Maley, & Brumfield, 2014). Average leaf area to perimeter ratio of each locality was calculated from the values obtained from ImageJ; input allele frequencies of the nextRAD markers were obtained using *STACKS*. All clines were fitted with three maximum-likelihood models: model I:  $p_{\min}/p_{\max}$  set to observed values without fitting exponential decay curves; model II:  $p_{\min}/p_{\max}$  estimated without fitting any decay curves; and model III:  $p_{\min}/p_{\max}$  estimated with decay curves at both ends fitted ( $p_{\min}$  and  $p_{\max}$  denote the lowest and highest average allele frequency in a locality detected for a marker, respectively). The model with the highest likelihood based on AIC scores was chosen for each marker. Cline centre, cline width, minimum and maximum allele frequency observed in each cline, and their two log likelihood (2lnL) support limits, were obtained using the same R package. From these measures, maximum change in allele frequency for each marker ( $\Delta p$ ) and cline slope ( $\Delta p/\text{width}$ ) were calculated.

An 'average' cline for molecular data was fitted using *STRUCTURE* ancestry scores for tests in cline coincidence (centre) and concordance (width); coincident or concordant clines

could mean similar environmental gradient was underlying them. Centres or width of all outlier clines and leaf dissection cline were re-fitted and fixed to those of the *STRUCTURE* cline. The decrease in 2lnL after fixing centre or width of each cline were tested using likelihood ratio tests, Bonferroni corrected for multiple tests. Clines were regarded as displaced or discordant with the *STRUCTURE* cline if the decrease in 2lnL was significant. Likelihood profiles for selected markers covering the observed range of cline centres and widths were also created (following Phillips, Baird, & Moritz, 2004).

### **Strength of selection**

A modified R script (original script provided by van Riemsdijk, Butlin, Wielstra, & Arntzen, 2019) was used to estimate the linkage disequilibrium, dispersal rate, and strength of selection in the hybrid zone. The average dispersal distance per generation ( $\sigma$ ) was obtained by  $\sqrt{rDw^2}$ , where  $r$  is recombination rate,  $D$  is linkage disequilibrium at hybrid zone centre,  $w$  is mean cline width of markers used; effective selection against hybrids ( $s$ ) was obtained by  $4\sigma^2/w^2$  (Barton & Hewitt, 1985; Szymura & Barton, 1986; 1991; Barton & Gale, 1993). Since recombination rate in the species is not known, a range of 0.1 to 0.5 was used. Forty markers with coincident and concordant clines were used in the estimation of selection (the biggest group of coincident and concordant clines in the dataset). These markers include the 33 markers in the elevational range of 1,900 – 2,000 m and with width around 1,200 m (as shown in Fig. 5) and those that are coincident and concordant with them (tested with LRT, using the average centre and width of the group of markers at 1,900 – 2,000 m). Mean and 95% confidence intervals (CI) for linkage disequilibrium and effective selection were calculated with 100 iterations of bootstrapping with replacement.

335

### 336 **Effect of selection on wider genomic regions**

337 To test whether the signal of selection in the outlier markers (with annotated adjacent genes)  
338 was detectable in a wide genomic region, non-outlier SNPs (contained in loci that did not show  
339 duplication in blast searches, with 95% base pair and 90% identity matched with genomic  
340 scaffolds) closest to the outlier SNPs on the same genomic scaffold were identified and their  
341  $F_{ST}$  values were compared to the outlier SNPs.

342

## 343 **Results**

344 To analyse genetic diversity and divergence among *Senecio* on Mount Etna, we conducted  
345 ‘nextRAD’ sequencing for a sample of 192 individuals from 18 localities across an elevational  
346 gradient on Mount Etna (Figure 1d). In total, we generated  $4.79 \times 10^8$  sequence reads that  
347 were mapped across 513,036 loci identified by *STACKS* (Catchen et al., 2011). Most of these  
348 loci (413,124) were invariable, while 99,427 loci contained at least one SNP. Out of these loci,  
349 1,769 SNPs with less than 50% missing data were used for analyses.

350

### 351 **Genetic diversity and structure of localities inferred from nextRAD dataset**

352 Various genetic diversity indices showed substantial variation (Table S1, Fig. S1). In general, *S.*  
353 *chrysanthemifolius* and low-elevation hybrid localities showed higher diversity than *S.*  
354 *aethnensis* and high-elevation hybrid sites. *S. chrysanthemifolius* and low-elevation localities  
355 showed generally a higher number of private alleles, a higher percentage of polymorphic loci,  
356 higher nucleotide diversity, a lower inbreeding coefficient ( $F_{IS}$ ), higher observed



heterozygosity and lower observed homozygosity (Table S1, Fig. S1). Pairwise  $F_{ST}$  increased with difference in elevation and geographic distance between localities (Fig. 3, Table S2).

After excluding SNPs with more than 50% missing data, 1,769 SNPs were retained for subsequent analyses. In the isolation by distance analysis, genetic distance had a stronger correlation with difference in elevation (Mantel test for genetic distance  $F_{ST}/(1-F_{ST})$ :  $r = 0.79$ ,  $P < 0.001$  in Fig. 3; pairwise  $F_{ST}$  matrix in Table S2) than geographic distance between locality pairs ( $r = 0.63$ ,  $p < 0.001$ ). Analysis of molecular variance (AMOVA) showed that most genetic variation is found among species or hybrid groupings (37.05%) and among individuals (58.98%) (Table 2). *STRUCTURE* and subsequent analyses revealed the optimal number of clusters ( $K$ ) is two (Fig. 1c; the same dataset but with the 76 SNP outliers excluded showed the same results thus results from the 1769-SNP dataset was used in all subsequent analyses). Most individuals at the two ends of the elevational gradient clustered into two distinct groups, each presumably representing one typical ('pure') species; admixed individuals were found at intermediate elevations, with a varying proportion of each cluster. There is a small amount of admixture detected in very high-elevation *S. aethnensis* samples, while very low-elevation *S. chrysanthemifolius* does not show any admixture. Principal components analysis (PCA; Fig 2) does not show conspicuous clustering of populations, but a gradual transition between high and low elevation samples. PC 1 shows high-elevation samples being more evenly distributed across the principal component while low-elevation ones are more clustered with several outliers in high-elevation samples' space. PC 2 shows rough clustering of each of the pure species and hybrids.

#### **Cline in leaf dissection**

The change in leaf area to perimeter ratio shows a clinal pattern (Fig. 4). The cline showed a rapid change in leaf area to perimeter ratio around the elevation of 1,900 m, with the cline centre estimated at 1,910 m ( $2\ln L = 1,882 - 1,935$  m), and the cline width of 127 m ( $2\ln L = 51 - 196$  m).

#### **Identification of outlier nextRAD markers and analysis of their clines**

To identify highly differentiated markers, we used *Arlequin* and *Bayescan*. The  $F_{ST}$  values, calculated for each SNP using *Arlequin*, ranged from 0 to 0.8587 (mean  $F_{ST} = 0.0854$ ). 183 SNPs were identified as outliers based on  $F_{ST}$  values (Fig. S3). *BayeScan* identified 89 SNPs with high  $F_{ST}$  and  $\log_{10}PO > 1$  (Fig S4), indicating they are likely to be under divergent selection.

A total of 76 SNPs were identified as outliers as they were significant in both outlier analyses. Distribution of these markers' maximum change in allele frequency, cline centre, cline width and cline slope are shown in Table S5 and Fig. S5. Cline centre positions showed a peak at 1,900 – 2,000 m (Fig. S5b). Cline width showed some variability (Fig. S5c), while cline slope ( $< 0.01$ ) were small for most markers (Fig. S5d). Cline width did not show correlation with cline centre position (Fig. S5e). However, clines centred at around 1,900 m showed especially steep slopes (Fig. S5f). The *STRUCTURE* cline, which acts as the 'average' cline for tests of coincidence and concordance, has a centre and width of 1852 m and 866 m respectively. Among the 76 outlier clines, 51 and 40 were coincident and concordant with the *STRUCTURE* cline respectively; while 18 were both coincident and concordant with the *STRUCTURE* cline (Table S4). These indicate that clines show significantly variable coincidence and concordance. In general, clines with more similar cline centres are more likely to be coincident. The leaf dissection cline is coincident but discordant with the *STRUCTURE* cline.

403

#### 404 **Potential association between outlier markers and functional genes**

405 Blast searches of outlier markers against scaffolds of unpublished *Senecio squalidus* draft  
406 genome and the non-redundant protein sequences database of NCBI led to the identification  
407 of 17 genes located within or in proximity (within 10 kb) of the markers (see Fig. 4 for clines;  
408 Table S3 for position of markers on scaffolds or distance from functional genes) associated  
409 with different functions. Some outlier genes' functions have no apparent association with  
410 adaptation to contrasting environments on Mount Etna; while other genes identified are  
411 involved in photosynthesis, defence response, photoperiodism, flowering, metal ion binding,  
412 and response to UV, which could underlie environmental or ecological adaptation, or  
413 reproductive isolation. The details about these genes, including blast results, outlier analyses  
414 results, cline statistics, gene annotations, and information about the markers nearest to these  
415 genes are summarised in Table S3.

416

#### 417 **Strength of selection**

418 Population linkage disequilibrium of the 40-marker dataset with coincident and concordant  
419 clines (Table S5) is elevated at the hybrid zone centre at around 1,900 – 2,000 m in elevation  
420 (Fig. S7). Linkage disequilibrium estimated for the cline centre is 0.3915 (95% CI = 0.3681 –  
421 0.4119). The dispersal rate was estimated to be 0.56 – 1.27 km/gen (corresponding to 144 –  
422 323 m in elevation) and the corresponding average effective selection is 0.1565 (95% CI =  
423 0.1472 - 0.1648) and 0.7831 (95% CI = 0.7521 - 0.8144), assuming recombination rate of 0.1  
424 and 0.5 respectively.

425

## **How wide are the genomic regions affected by divergent selection?**

Identifying non-outlier SNPs (noSNPs) that are closest to the 17 outliers (oSNPs) through blasting of adjacent regions (same criteria as identifying genomics scaffolds for outliers), it was revealed that the distance between the noSNPs and oSNPs (that fall within the same scaffold) range from around 50 kb to 1.3 mb, with  $F_{ST}$  for noSNPs ranging from 0 to 0.19. For some genomic regions, noSNPs with  $F_{ST}$  less than 0.047 are located as close as 51 kb to oSNPs (e.g. marker 10586 in Table S3); while in other regions, the distance was much longer and the noSNP's  $F_{ST}$  was not as low (e.g. 400 kb and  $F_{ST} = 0.20$  for marker 185 in Table S3). This indicates that the signal of selection in the genomes of Etnean *Senecio* species may be very localised. Further work has to be done to study the selection patterns (and evaluate the effect of missing data) in detail.

## **Demographic history of *Senecio* on Mount Etna**

We first focused on the analysis of demographic history between the pure species, as done in our previous work (Filatov et al., 2016). That previous work was focusing on overall species demography and did not consider the possibility that different parts of the genome may have different rates of interspecific gene flow due to selection preventing introgression of some genomic regions. To take the possibility of heterogeneous gene flow across the genome into account, we allowed an *IM* model to have two bi-directional migration parameters,  $M_A$  and  $M_B$  (model *IM2M*, Figure 6a). The *IM2M* model fits data significantly better than the models without heterogeneous migration (AIC score = 399.04; Table 3, Fig. 6a). Another model, *SC\_IM2M*, was almost as likely (AIC score = 399.14; Table 3, Fig 6b). Both models involve heterogeneous gene flow, with the higher migration rates being 4.38 and 4.96 times larger

than the other lower ones for the models *IM2M* and *SC\_IM2M* respectively. Likelihood ratio tests (LRT) were carried out for five groups of nested models. The LRT between *IMpre* and *IM* models was not significant (p-value = 0.57), indicating that allowing for an ancestral population size change prior to species split (in model *IMpre*) does not significantly improve the fit to data. LRT for other four model comparisons were significant. In particular, allowing for migration dramatically improves the fit to data compared to the nested model without migration (*split\_mig* versus *split*, p-value =  $1.76 \times 10^{-30}$ ). Allowing migration in both directions significantly improves the fit to data compared to unidirectional migration (*IM* versus *IM1* or *IM2*, p-value =  $5.55 \times 10^{-13}$  and  $3.74 \times 10^{-16}$  respectively). Having two separate classes of bi-directional migration significantly improves model fit compared to only one class of migration (*IM2M* versus *IM2M\_1*, p-value = 0.0066). These results indicate that the genomes are experiencing gene flow in both directions and that gene flow is heterogeneous (i.e. a fraction of the genome is exchanging alleles significantly less than the rest of the genome). Although the models assuming heterogeneous gene flow did not test for symmetry of gene flow in each class, results from models with separate parameters for different directions of migration (*IM*, *IMpre*, *SC*, *eSC*; see Table 3) suggest that gene flow in the same class is slightly asymmetric. Migration rate from *S. chrysanthemifolius* to *S. aethnensis* is 1.24 to 1.70 times higher than from *S. chrysanthemifolius* to *S. aethnensis*.

The best fitting model (*IM2M*) was also fitted to data from other pairwise comparisons of species and hybrid groups to investigate different demographic parameters at a finer scale. Another isolation with migration model, *IM*, was also run to assess the relative amount of gene flow in each direction in different comparisons (see parameters in Table 3). All groups show smaller current population sizes compared to their ancestral sizes. In all species/hybrid

comparisons (C/LH, C/HH, A/LH, A/HH, where C = *S. chrysanthemifolius*, A = *S. aethnensis*, LH – low-elevation hybrids and HH = high-elevation hybrids) under the model *IM2M*, one class of migration is always at least twice (2.3 to 8.5 times) larger than the other one. Migration is also higher between localities that are closer to each other (C/LH and A/HH) than those further apart (C/HH and A/LH). Under the *IM* model, the migration rate from the pure species to hybrids ( $M_{21}$ ) is 1.6 to 3 times larger than that in the opposite direction ( $M_{12}$ ).

In the high- and low-elevation hybrids comparison (HH/LH), the two classes of migration rate are both high under the model *IM2M* (3.61 and 2.26) and *IM* (3.72 and 3.04), likely indicating most of their genomes share genes more freely (instead of having regions with restricted gene flow).

## Discussion

Hybrid zones are a powerful tool to study the dynamics of phenotypic and genotypic divergence between closely related species; also, recently diverged species offer great opportunities to catch ‘speciation in action’ by studying the patterns of gene flow and genomic heterogeneity in taxa subject to divergent selection (Via, 2009). *S. aethnensis* and *S. chrysanthemifolius* on Mount Etna are characterised by a hybrid zone and recent divergence less than 200,000 years ago. Using genome-wide SNPs in samples comprising both species and their hybrids, we investigated demographic features, patterns of gene flow and selection in this system, and factors that are likely contributing to maintenance of divergence in the face of on-going gene flow between the two species.

## Demographic history of speciation in Etnean *Senecio*

Various demographic models implemented in *dadi* (see Fig. S2 for visualisation of models) were used to reconstruct the most likely speciation scenario and demographic features in the divergence of *S. aethnensis* and *S. chrysanthemifolius* on Mount Etna.

Our analysis revealed that the *IM2M* model fits the data best. This model has not been considered in previous studies in *Senecio*, but some of the parameter estimates are similar to that obtained previously. In particular, migration between the two pure species inferred here is similar to the estimate from the most likely model in Filatov et al. (2016), which is less than one migrant per generation on average (average between  $M_A$  and  $M_B$ ; number of migrants per generation is higher in geographically closer comparisons in the current study). Given models with (*SC\_IM2M*) and without (*IM2M*) secondary contact both have high relative likelihoods, there is little power in the data to distinguish between these demographic scenarios; it may also be seen as a lack of evidence for the secondary contact scenario as the more complex *SC\_IM2M* model did not significantly improve fit to data (consistent with Filatov et al.; 2016). What is common between both models is that they both involve heterogeneous gene flow. This indicates that a fraction of the genome introgresses considerably slower compared to the rest of the genome, possibly due to intrinsic or extrinsic selection against introgressed alleles in these regions. Many studies have demonstrated heterogeneous divergence in different genomes and that divergent selection has a crucial role in genomic heterogeneity (reviewed in Nosil, Funk, & Ortiz-Rrientos, 2009). Through demographic modelling, we have shown that heterogeneous gene flow is indeed a feature in Etnean *Senecio*.

Another interesting point to note is that gene flow is highly asymmetric, as revealed by four models for the pure species comparison and *IM* analyses of other pure species/ hybrid comparisons. Gene flow from *S. chrysanthemifolius* to *S. aethnensis* is 1.24 to 1.70 times

higher than the other way around; while gene flow is always (1.6 to 3 times) greater from pure species to hybrids, compared to gene flow from hybrids to pure species. This low rate of introgression from hybrid to pure species could be caused by various reasons, such as lower reproductive fitness in hybrids, and low rate of backcrossing. The directionality of gene flow helps to explain the apparent contradiction between plentiful evidence of hybridisation at intermediate elevations and relatively modest estimates of gene flow between the pure species at the two extremes of the elevational cline.

#### **Variable coincidence and concordance among phenotypic and genotypic clines**

We fitted clines for leaf dissection and genetic markers using the same individuals. Likelihood ratio tests revealed that clines have significantly variable coincidence and concordance. Although clines studied here have variable coincidence, they are all centred in the putative hybrid zone (1,200 – 2,000 m in elevation), with only a few exceptions that are centred above 2000 m (this corresponds to the observation in the *STRUCTURE* analysis where there is a little admixture in high-elevation *S. aethnensis*). These environmental and ecological factors likely vary in different ways with regard to elevations within the hybrid zone. Other studies, such as those on the marine snails *Littorina saxatilis*, have also suggested displaced clines among different environmental transitions that would lead to selection acting on different loci independently (e.g. Hollander, Galindo, & Butlin, 2015). Like the current study, many studies on these snails have also identified genomic regions under divergent selection and associated with adaptive phenotypic traits (Hollander et al., 2015; Pennec et al., 2017; Westram et al., 2014).



Analysing allozymes, simple sequence repeats (SSR) and various groups of phenotypic measurements, Brennan et al. (2009) found highly coincident and concordant clines among all of them, in which they are centred at 6.67 – 7.82 km (corresponding to elevations somewhere between 1,515 – 1,928 m) with widths of 1.49 – 3.7 km. In particular, they found the leaf structure cline to be centred at 6.67 (6.25 – 6.97) km with width of 1.49 (0.06 – 2.39) km. These support limits translate into cline centre within the elevational range of 1,515 – 1,795 m and width of more than 400 m in elevation. Brennan et al. (2009)'s leaf structure cline does not seem to be coincident with the leaf dissection cline in this study, while the cline width in this study is well within the range reported by Brennan et al. (2009) [in the current study, cline centre = 1,910 (1,882 – 1,935) m; width = 127 (51 – 196 m)]. The discrepancy could be due to: 1) more than one leaf traits were combined in the leaf structure cline in Brennan et al. (2009). Individual leaf trait clines might have centres and widths different from leaf dissection; 2) samples in Brennan et al. (2009) were collected from a few areas located on different sides of Mount Etna, while samples in this study were collected along a more or less straight transect on the southern side of the mountain. Hence, results in the two studies should be compared with caution.

#### **Strong selection against hybrids on Mount Etna**

Effective selection against hybrids inferred in this study (0.16 – 0.78 assuming recombination between the markers is  $r = 0.1 - 0.5$ ) is much higher than that in Brennan et al. (2009) (0.02 – 0.11 for  $r = 0.1 - 0.5$  respectively) for the same species. Dispersal rate inferred in this study (0.56 – 1.27 km/gen for  $r = 0.1 - 0.5$ ) is also greater than that in Brennan et al. (2009) (0.17 – 0.38 km/gen for  $r = 0.1 - 0.5$ ). Both studies used only coincident and concordant clines in

estimating selection, thus the difference could be related to the type of markers used (allozymes and microsatellites in Brennan et al. (2009); SNPs in the current study). For instance, microsatellites have multiple alleles, hence higher heterozygosities and mutation rate than SNPs (Mueller, 2004); these properties could lead to different estimates of linkage disequilibrium and subsequent estimates. In our analysis, linkage disequilibrium is elevated at the hybrid zone centre, which is expected for a hybrid zone experiencing strong selection. However, linkage disequilibrium in the high-elevation localities for *S. aethnensis* is also quite high. This could be caused by an influx of alleles from *S. chrysanthemifolius*, as revealed by the presence of admixed individuals in high-elevation localities in the *STRUCTURE* analysis, and asymmetric migration in demographic modelling.

Estimates of selection and dispersal from a recombination rate of 0.5 (the higher values) are probably closer to reality as it is unlikely that all markers used are tightly clustered. Our selection estimate from this recombination rate corresponds to a 78% drop in fitness in hybrids in the centre of hybrid zone, which indicates that the *Senecio* cline is maintained by fairly strong selection. This is one of the highest estimates reported (Table 1). Previous studies on salamanders (Alexandrino et al., 2005) and skinks (Phillips et al., 2004) have reported values similar to the current study, yet they calculated selection using  $s = 8\sigma^2/w^2$  while our study used  $s^* = 4\sigma^2/w^2$  (Table 1;  $s^* = 4\sigma^2/w^2$  measures the difference in mean fitness between centre and edge of hybrid zone, and measuring this difference in mean fitness makes selection estimates comparable between different forms of selection; whereas  $s = 8\sigma^2/w^2$  assumes half of the individuals are heterozygotes at the hybrid zone centre, where  $s = 2s^*$ ). In other words, estimate in the current study (0.78) is at least two, and up to more than 200, times larger than that in other recent studies presented in Table 1 after accounting for the fold differences in

the formulae used. It is worth noting that Brennan et al. (2009) also calculated effective selection in Etnean *Senecio* with  $8\sigma^2/w^2$ , though this does not account for the difference between the estimates in their and the current studies either.

The inferred dispersal (0.56 – 1.27 km/gen) is rather small, compared to what one would expect for wind-dispersed herbaceous plants. This, together with strong selection against hybrids and demographic modelling showing around one migrant per generation, collectively indicate that gene flow is restricted, likely due to divergent selection. Selection against hybrids has only been shown to manifest as hybrid breakdown in  $F_2$  plants in two crosses in two studies (Brennan et al., 2014; Chapman et al., 2016), thus larger-scale studies are required to further investigate the effect on hybrid establishment and fitness. Multifarious selection is evident in this system, as clines of many outlier markers are relatively wide (hence selection at many individual traits is unlikely to be strong) while a few show rather narrow clines with widths under 100 m; and only a small proportion of clines is coincident and concordant. The strong selection against hybrids and occurrence of multifarious selection likely facilitates local adaptation in the two species and their divergence. Future work that analyses how potential environmental or ecological selective forces (for example, whether they change gradually or abruptly along the gradient and how different their effects are) had shaped the system would be particularly fascinating for this young but complex system.

#### **Intrinsic and extrinsic causes in the divergence of Etnean *Senecio***

Regardless of the speciation scenario at the start of divergence, Etnean *Senecio* has experienced heterogeneous gene flow. One question that arises from this is whether selective sweeps [leading to (near-) fixation of SNPs in populations of pure species] or barriers to gene

flow (selection in the hybrid zone in this case) cause divergence in this differentiated portion of genome (Tavares et al., 2018). Both of these would show signatures of divergent selection, and disentangling between the two would require higher-resolution genomic data. It would also be interesting to quantify the regions and extent of frequent or rare migration in the genome in future studies.

Research on intrinsic incompatibilities is often disconnected from studies of extrinsic selection, making integrating different components of reproductive isolation challenging (Seehausen et al., 2014). With both intrinsic incompatibility and multifarious divergent selection, the Etnean *Senecio* allows one to combine both directions of research to study the interplay between intrinsic and extrinsic processes. This adds to the limited literature in other systems which also have evidence for both, including in killfish, *Lucania*, where there is extrinsic isolation caused by salinity and intrinsic incompatibilities (Fuller, 2008); and in the copepod *Tigriopus californicus*, where interpopulation hybrids show adaptation to different thermal conditions and intrinsic incompatibilities (Ellison & Burton, 2006, 2008; Willett, 2010). However, unlike these systems, the Etnean *Senecio* is parapatric and multifarious selection might be crucial in creating strong enough reproductive isolation to allow the accumulation and maintenance of genetic divergence in the system (Seehausen et al., 2014).

#### **Maintenance of divergence despite gene flow**

It is intriguing how the pair of sister *Senecio* species maintain their divergence while hybridising in the relatively small area of Mount Etna. Yet, this phenomenon is not uncommon - *Quercus* (oaks) and *Populus* (poplars) are well-studied groups with a 'porous' species boundary. Studies in these two groups have shown that their species identities are maintained

by an array of mechanisms, some of which have been presented or observed in the Etnean *Senecio*. These include, in oaks, divergent selection (Ortego, Gugger, & Sork, 2017; Scotti-Saintagne et al., 2004), and asynchrony in flowering leading to assortative mating (Gailing & Curtu, 2014); in poplars, intrinsic incompatibility (Christe et al., 2017; Roe et al., 2014), and selection against hybrids (Christe et al., 2016). It is plausible that a combination of divergent selection, strong cumulative selection against hybrids and difference in phenology (such as flowering times) helps to reinforce the reproductive isolation in the system. Given the prevalence of hybridisation between closely-related plant species across different families, these systems point to the possibility that more unstudied plant groups and species complexes might have extensive hybridisation while maintaining their respective species boundaries or divergence at the sub-species levels. Studying these groups would greatly benefit the field of plant hybridisation, speciation with gene flow, and study of the role of gene flow, selection and introgression in adaptation and speciation.

## **Conclusion**

In this study, we have shown that only a small proportion of differentiated loci (76 out of 1,769 studied) and strong cumulative multifarious selection at a handful of genes are likely involved in keeping the two Etnean *Senecio* species distinct. Although the exact mechanism of speciation in this system is far from clear, this study has added to the body of evidence that both intrinsic and extrinsic processes have roles in speciation and maintenance of divergence in the face of gene flow (Ellison & Burton, 2006, 2008; Fuller, 2008; Willett, 2010). To summarise, we have 1) shown heterogeneous, bidirectional gene flow, and population size changes in the past are characteristics of the speciation of Etnean *Senecio*; 2) discovered

promising candidate genes that are potentially linked to local adaptation; 3) inferred the likely presence of multifarious selective forces of different strengths; and 4) estimated strong selection against hybrids. It is crucial to extend this work by identifying the selective forces underlying divergence and linking them to elevation or ecology, analysing fine-scale genomic patterns that harbour regions of interests, the interplay between intrinsic incompatibilities and extrinsic, multifarious environmental selection in shaping the system, and the potential role of other genetic phenomena (such as genetic hitchhiking and chromosomal rearrangement) in causing divergence.

## Acknowledgements

This work was funded by grants to DAF from NERC and BBSRC. We would like to thank Isolde van Riemsdijk (NCB Naturalis) and Prof. Roger Butlin (University of Sheffield and University of Gothenburg) for kindly providing and helping to modify the R script and discussion of the relevant analyses. We are also grateful for Prof. Roger Butlin and anonymous reviewers for providing comments on the manuscript.

## References

- Alboukadel, K., & Fabian, M. (2017). factoextra: Extract and Visualize the Results of Multivariate Data Analyses.
- Alexandrino, J., Baird, S. J., Lawson, L., Macey, R. J., Moritz, C., & Wake, D. B. (2005). Strong selection against hybrids at a hybrid zone in the *Ensatina* ring species complex and its evolutionary implications. *Evolution*, 59(6), 1334–1347. doi:10.1554/04-156
- Antonovics, J., & Bradshaw, A. D. (1970). Evolution in closely adjacent plant populations VIII. Clinal patterns at a mine boundary. *Heredity*, 25(3), 349–362. doi:10.1038/hdy.1970.36
- Bailey, R. I., Tesaker, M. R., Trier, C. N., & Sætre, G.-P. (2015). Strong selection on male plumage in a hybrid zone between a hybrid bird species and one of its parents. *Journal of Evolutionary Biology*, 28(6), 1257–1269. doi:10.1111/jeb.12652

- Baldassarre, D. T., White, T. A., Karubian, J., & Webster, M. S. (2014). Genomic and morphological analysis of a semipermeable avian hybrid zone suggests asymmetrical introgression of a sexual signal. *Evolution*, 68(9), 2644–2657. doi:10.1111/evo.12457
- Barton, N. H., & Gale, K. S. (1993). Genetic analysis of hybrid zones. In: pp. 13–45. Oxford University Press.
- Barton, N. H., & Hewitt, G. M. (1985). Analysis of Hybrid Zones. *Annual Review of Ecology and Systematics*, 16(1), 113–148.
- Bohonak, A. J. (2002). IBD (Isolation by Distance): A Program for Analyses of Isolation by Distance. *Journal of Heredity*, 93, 153–154. doi:10.1093/jhered/93.2.153
- Bougeard, S., & Dray, S. (2018). Supervised Multiblock Analysis in R with the ade4 Package. *Journal of Statistical Software*, 86(1). doi:10.18637/jss.v086.i01
- Brelsford, A., & Irwin, D. (2009). Incipient Speciation Despite Little Assortative Mating: The Yellow-Rumped Warbler Hybrid Zone. *Evolution*, 63(12), 3050–3060. doi:10.1111/j.1558-5646.2009.00777.x
- Brennan, A. C., Bridle, J. R., Wang, A.-L., Hiscock, S. J., & Abbott, R. J. (2009). Adaptation and selection in the *Senecio* (Asteraceae) hybrid zone on Mount Etna, Sicily. *The New phytologist*, 183, 702–17. doi:10.1111/j.1469-8137.2009.02944.x
- Brennan, A. C., Hiscock, S. J., & Abbott, R. J. (2014). Interspecific crossing and genetic mapping reveal intrinsic genomic incompatibility between two *Senecio* species that form a hybrid zone on Mount Etna, Sicily. *Heredity*, 113, 195–204. doi:10.1038/hdy.2014.14
- Brennan, A. C., Hiscock, S. J., & Abbott, R. J. (2016). Genomic architecture of phenotypic divergence between two hybridizing plant species along an elevational gradient. *AoB PLANTS*, 8, plw022. doi:10.1093/aobpla/plw022
- Brennan, A. C., Hiscock, S. J., & Abbott, R. J. (2019). Completing the hybridization triangle: the inheritance of genetic incompatibilities during homoploid hybrid speciation in ragworts (*Senecio*). *AoB PLANTS*, 11(1), ply078. doi:10.1093/aobpla/ply078
- Carneiro, M., Baird, S., Afonso, S., Ramirez, E., Tarroso, P., Teotónio, H., ... Ferrand, N. (2013). Steep clines within a highly permeable genome across a hybrid zone between two subspecies of the European rabbit. *Molecular Ecology*, 22(9), 2511–2525. doi:10.1111/mec.12272
- Catchen, J. M., Amores, A., Hohenlohe, P., Cresko, W., & Postlethwait, J. H. (2011). Stacks: Building and Genotyping Loci De Novo From Short-Read Sequences. *G3: Genes, Genomes, Genetics*, 1, 171–182. doi:10.1534/g3.111.000240
- Chapman, M. A., Forbes, D. G., & Abbott, R. J. (2005). Pollen competition among two species of *Senecio* (Asteraceae) that form a hybrid zone on Mount Etna, Sicily. *American journal of botany*, 92, 730–735. doi:10.3732/ajb.92.4.730
- Chapman, M. A., Hiscock, S. J., & Filatov, D. A. (2013). Genomic Divergence during Speciation Driven by Adaptation to Altitude. *Molecular Biology and Evolution*, 30, 2553–2567. doi:10.1093/molbev/mst168
- Chapman, M. A., Hiscock, S. J., & Filatov, D. A. (2016). The genomic bases of morphological divergence and reproductive isolation driven by ecological speciation in *Senecio* (Asteraceae). *Journal of Evolutionary Biology*, 29, 98–113. doi:10.1111/jeb.12765
- Chessel, D., Dufour, A., & Thioulouse, J. (2004). The ade4 Package - I: One-Table Methods. *R News*, 4(1), 5–10.

- Christe, C., Stölting, K., Bresadola, L. *et al.* (2016). Selection against recombinant hybrids maintains reproductive isolation in hybridizing *Populus* species despite F<sub>1</sub> fertility and recurrent gene flow. *Molecular Ecology*, 25, 2482–2498. doi.org/10.1111/mec.13587
- Christe, C., Stölting, K., Paris, M. *et al.* (2017). Adaptive evolution and segregating load contribute to the genomic landscape of divergence in two tree species connected by episodic gene flow. *Molecular Ecology*, 26, 59–76. doi:10.1111/mec.13765
- Daroski, H., Feder, J. (2007). Host plant and latitude-related diapause variation in *Rhagoletis pomonella*: a test for multifaceted life history adaptation on different stages of diapause development. *Journal of Evolutionary Biology*, 20, 2101–2112. doi:10.1111/j.1420-9101.2007.01435.x
- Delmore, K., & Irwin, D. (2014). Hybrid songbirds employ intermediate routes in a migratory divide. *Ecology Letters*, 17(10), 1211–1218. doi.org/10.1111/ele.12326
- Derryberry, E. P., Derryberry, G. E., Maley, J. M., & Brumfield, R. T. (2014). hzar: hybrid zone analysis using an R software package. *Molecular Ecology Resources*, 14, 652–663. doi:10.1111/1755-0998.12209
- Doyle, J. J., & Doyle, J. (1987). A rapid DNA isolation procedure for small quantities of fresh leaf tissue. *Phytochemistry Bulletin*, 19, 11–15.
- Dray, S., Dufour, A., & Chessel, D. (2007). The ade4 Package - II: Two-Table and K-Table Methods. *R News*, 7(2), 47–52. doi:10.18637/jss.v022
- Dray, S., & Dufour, A. (2007). The ade4 Package: Implementing the Duality Diagram for Ecologists. *Journal of Statistical Software*, 22(4), 1–20.
- Durrett, R., Buttell, L., & Harrison, R. (2000). Spatial models for hybrid zones. *Heredity*, 84(1), 6885660. doi:10.1046/j.1365-2540.2000.00566.x
- Earl, D. A., & vonHoldt, B. M. (2012). STRUCTURE HARVESTER: a website and program for visualizing STRUCTURE output and implementing the Evanno method. *Conservation Genetics Resources*, 4, 359–361. doi:10.1007/s12686-011-9548-7
- Egea-Serrano, A., Hangartner, S., Laurila, A., Räsänen, K. (2014). Multifarious selection through environmental change: acidity and predator-mediated adaptive divergence in the moor frog (*Rana arvalis*). *Proceedings of the Royal Society B: Biological Sciences*, 281, 20133266. doi:10.1098/rspb.2013.3266
- Ellison, C. K., Burton, R. S. (2006). Disruption of mitochondrial function in interpopulation hybrids of *Tigriopsis californicus*. *Evolution*, 60, 1382–1391. doi:10.1554/06-210.1
- Ellison, C. K., Burton, R. S. (2008). Interpopulation hybrid breakdown maps to the mitochondrial genome. *Evolution*, 62, 631–638. doi:10.1111/j.1558-5646.2007.00305.x
- Evanno, G., Regnaut, S., & Goudet, J. (2005). Detecting the number of clusters of individuals using the software structure: a simulation study. *Molecular Ecology*, 14, 2611–2620. doi:10.1111/j.1365-294X.2005.02553.x
- Excoffier, L., Laval, G., & Schneider, S. (2005). Arlequin (version 3.0): An integrated software package for site genetics data analysis. *Evolutionary Bioinformatics*, 1, 117693430500100003. doi:10.1177/117693430500100003
- Feder, J. L., Egan, S. P., & Nosil, P. (2012). The genomics of speciation-with-gene-flow. *Trends in Genetics*, 28, 342–350. doi:10.1016/j.tig.2012.03.009
- Filatov, D. A., Osborne, O. G., & Papadopoulos, A. S. T. (2016). Demographic history of speciation in a *Senecio* altitudinal hybrid zone on Mount Etna. *Molecular Ecology*, 25, 2467–2481. doi:10.1111/mec.13618



771 Foll, M., & Gaggiotti, O. (2008). A genome-scan method to identify selected loci appropriate  
 772 for both dominant and codominant markers: a Bayesian perspective. *Genetics*, 180,  
 773 977–93. doi:10.1534/genetics.108.092221

774 Fuller, R. C. (2008). Genetic incompatibilities in killfish and the role of environment. *Evolution*,  
 775 62, 3056–3068. doi:10.1111/j.1558-5646.2008.00518.x

776 Gailing, O., Curtu, A. (2014). Interspecific gene flow and maintenance of species integrity in  
 777 oaks. *Annals of Forest Research*, 0, 1–14. doi:10.15287/afr.2014.171

778 Gompert, Z., Lucas, L., Nice, C. et al. (2013). Geographically multifarious phenotypic  
 779 divergence during speciation. *Ecology and Evolution*, 3, 595–613. doi:10.1002/ece3.445

780 Gutenkunst, R. N., Hernandez, R. D., Williamson, S. H., & Bustamante, C. D. (2009). Inferring  
 781 the Joint Demographic History of Multiple Sites from Multidimensional SNP Frequency  
 782 Data. *PLoS Genetics*, 5, e1000695. doi:10.1371/journal.pgen.1000695

783 Hollander, J., Galindo, J., & Butlin, R. K. (2015). Selection on outlier loci and their association  
 784 with adaptive phenotypes in *Littorina saxatilis* contact zones. *Journal of Evolutionary  
 785 Biology*, 28(2), 328–337. doi:10.1111/jeb.12564

786 James, J. K., & Abbott, R. J. (2005). Recent, allopatric, homoploid hybrid speciation: the origin  
 787 of *Senecio squalidus* (Asteraceae) in the British Isles from a hybrid zone on Mount Etna,  
 788 Sicily. *Evolution*, 59(12):2533–2547. doi:10.1554/05-306.1

789 Kawakami, T., Butlin, R. K., Adams, M., Paull, D. J., & Cooper, S. J. (2009). Genetic analysis of a  
 790 chromosomal hybrid zone in the Australian morabine grasshoppers (*Vandiemenella*,  
 791 *Viatica* species group). *Evolution*, 63(1), 139–152. doi.org/10.1111/j.1558-  
 792 5646.2008.00526.x

793 Kruuk, L. E., Baird, S. J., Gale, K. S., & Barton, N. H. (1999). A comparison of multilocus clines  
 794 maintained by environmental adaptation or by selection against hybrids. *Genetics*,  
 795 153(4), 1959–71.

796 Körner, C. (2007). The use of “altitude” in ecological research. *Trends in Ecology & Evolution*,  
 797 22, 569–574. doi:10.1016/j.tree.2007.09.006

798 Macholn, M., Munclinger, P., Šugerkov, M., Dufkov, P., Bmov, B., Božkov, E., ... Pilek, J. (2007).  
 799 Genetic analysis of autosomal and X-linked markers across a mouse hybrid zone.  
 800 *Evolution*, 61(4), 746–771. doi.org/10.1111/j.1558-5646.2007.00065.x

801 Mallet, J. (2005). Hybridization as an invasion of the genome. *Trends in Ecology & Evolution*,  
 802 20, 229–37. doi:10.1016/j.tree.2005.02.010

803 Mueller, J. (2004). Linkage disequilibrium for different scales and applications. *Briefings in  
 804 Bioinformatics*, 5(4), 355–364. doi:10.1093/bib/5.4.355

805 Muir, G., Osborne, O., Sarasa, J., Hiscock, S., & Filatov, D. (2013). Recent ecological selection  
 806 on regulatory divergence is shaping clinal variation in *Senecio* on Mount Etna. *Evolution*,  
 807 67, 3032–3042. doi:10.1111/evo.12157

808 Nevado, B., Contreras-Ortiz, N., Hughes, C., & Filatov, D. A. (2018). Pleistocene glacial cycles  
 809 drive isolation, gene flow and speciation in the high-elevation Andes. *New Phytologist*,  
 810 219, 779–793. doi:10.1111/nph.15243

811 Nosil, P., Funk, D. J., & Ortiz-Barrientos, D. (2009). Divergent selection and heterogeneous  
 812 genomic divergence. *Molecular Ecology*, 18(3), 375–402. doi:10.1111/j.1365-  
 813 294X.2008.03946.x

814 Nosil, P., Harmon, L., Seehausen, O. (2009) Ecological explanations for (incomplete) speciation.  
 815 *Trends in Ecology & Evolution*, 24, 145–156. doi:10.1016/j.tree.2008.10.011

- Ortego, J., Gugger, P., Sork, V. (2017). Impacts of human-induced environmental disturbances on hybridization between two ecologically differentiated Californian oak species. *New Phytologist*, 213, 942–955. doi:10.1111/nph.14182
- Osborne, O., Batstone, T. E., Hiscock, S. J., & Filatov, D. A. (2013). Rapid Speciation with Gene Flow Following the Formation of Mount Etna. *Genome Biology and Evolution*, 5, 1704–1715. doi:10.1093/gbe/evt127
- Phillips, B. L., Baird, S. J., Moritz, C. (2004). When vicars meets: a narrow contact zone between morphologically cryptic phylogeographic lineages of the Rainforest Skink, *Carlia Rubrigularis*. *Evolution*, 58, 1536–1548. doi:10.1111/j.0014-3820.2004.tb01734.x
- Polyakov, A. V., White, T. A., Jones, R. M., Borodin, P. M., & Searle, J. B. (2011). Natural hybridization between extremely divergent chromosomal races of the common shrew (*Sorex araneus*, Soricidae, Soricomorpha): hybrid zone in Siberia. *Journal of Evolutionary Biology*, 24(7), 1393–1402. doi:10.1111/j.1420-9101.2011.02266.x
- Pritchard, J., Stephens, M., & Donnelly, P. (2000). Inference of site structure using multilocus genotype data. *Genetics*, 155, 945–59.
- Roe, A., MacQuarrie, C., Gros-Louis, M. et al. (2014). Fitness dynamics within a poplar hybrid zone: I. Prezygotic and postzygotic barriers impacting a native poplar hybrid stand. *Ecology and Evolution*, 4, 1629–1647. doi:10.1002/ece3.1029
- Ross, R.I. (2010). Local adaptation and adaptive divergence in a hybrid species complex in *Senecio* (Unpublished doctoral dissertation). Univeristy of Oxford.
- Russello, M. A., Waterhouse, M. D., Etter, P. D., & Johnson, E. A. (2015). From promise to practice: pairing non-invasive sampling with genomics in conservation. *PeerJ*, 3, e1106. doi:10.7717/peerj.1106
- Schneider, C. A., Rasband, W. S., & Eliceiri, K. W. (2012). NIH Image to ImageJ: 25 years of image analysis. *Nature Methods*, 9, nmeth.2089. doi:10.1038/nmeth.2089
- Scotti-Saintagne, C., Mariette, S., Porth, I. et al. (2004). Genome Scanning for Interspecific Differentiation Between Two Closely Related Oak Species [*Quercus robur* L. and *Q. petraea* (Matt.) Liebl.]. *Genetics*, 168, 1615–1626. doi:10.1534/genetics.104.026849
- Seehausen, O., Butlin, R. K., Keller, I., Wagner, C. E., Boughman, J. W., Hohenlohe, P. A., ... Saetre, G.-P. (2014). Genomics and the origin of species. *Nature Reviews Genetics*, 15, 176–192. doi:10.1038/nrg3644
- senecioDB. (undated). senecioDB: A genomic resource for *Senecio* species. Retrieved from [http://www.seneciodb.org/wordpress/?page\\_id=22](http://www.seneciodb.org/wordpress/?page_id=22).
- Singhal, S., & Moritz, C. (2012). Strong selection against hybrids maintains a narrow contact zone between morphologically cryptic lineages in a rainforest lizard. *Evolution*, 66(5), 1474–1489. doi.org/10.1111/j.1558-5646.2011.01539.x
- Sobel, J., Stankowski, S., Streisfeld, M. (2019). Variation in ecophysiological traits might contribute to ecogeographic isolation and divergence between parapatric ecotypes of *Mimulus aurantiacus*. *Journal of Evolutionary Biology*, 32, 604–618. doi:10.1111/jeb.13442
- Stankowski, S., Sobel, J. M., & Streisfeld, M. A. (2017). Geographic cline analysis as a tool for studying genome-wide variation: a case study of pollinator-mediated divergence in a monkeyflower. *Molecular ecology*, 26, 107–122. doi:10.1111/mec.13645

- Tavares, H., Whibley, A., Field, D. L., Bradley, D., Couchman, M., Copsey, L., ... Coen, E. (2018). Selection and gene flow shape genomic islands that control floral guides. *Proceedings of the National Academy of Sciences*, 115(43), 201801832. doi:10.1073/pnas.1801832115
- Teeter, K. C., Payseur, B. A., Harris, L. W., Bakewell, M. A., Thibodeau, L. M., O'Brien, J. E., ... Tucker, P. K. (2008). Genome-wide patterns of gene flow across a house mouse hybrid zone. *Genome Research*, 18, 67–76. doi:10.1101/gr.6757907
- Tine, M., Kuhl, H., Gagnaire, P.-A., Louro, B., Desmarais, E., Martins, R., ... Reinhardt, R. (2014). European sea bass genome and its variation provide insights into adaptation to euryhalinity and speciation. *Nature Communications*, 5, 5770. doi:10.1038/ncomms6770
- van Riemsdijk, I., Butlin, R. K., Wielstra, B., & Arntzen, J. W. (2019). Testing an hypothesis of hybrid zone movement for toads in France. *Molecular Ecology*, 28(5), 1070–1083. doi:10.1111/mec.15005
- Via, S. (2009). Natural selection in action during speciation. *Proceedings of the National Academy of Sciences*, 106(Supplement 1), 9939–9946. doi:10.1073/pnas.0901397106
- Vines, T., Dalziel, A., Albert, A., Veen, T., Schulte, P., & Schluter, D. (2016). Cline coupling and uncoupling in a stickleback hybrid zone. *Evolution*, 70(5), 1023–1038. doi.org/10.1111/evo.12917
- Wielstra, B., Burke, T., Butlin, R., Avci, A., Üzümlü, N., Bozkurt, E., ... Arntzen, J. (2017). A genomic footprint of hybrid zone movement in crested newts. *Evolution Letters*, 1(2), 93–101. doi:10.1002/evl3.9
- Willett, C. S. (2010). Potential fitness trade-offs for thermal tolerance in the intertidal copepod *Tigriopsis californicus*. *Evolution*, 64, 2521–2534. doi:10.1111/j.1558-5646.2010.01008.x
- Wu, C. (2001). The genic view of the process of speciation. *Journal of Evolutionary Biology*, 14, 851–865. doi:10.1046/j.1420-9101.2001.00335.x
- Young, N. D. (1996). Concordance and discordance: a tale of two hybrid zones in the pacific coast irises (Iridaceae). *American Journal of Botany*, 83(12), 1623–1629. doi:10.1002/j.1537-2197.1996.tb12820.x

## Data Accessibility Statement

All sequences were submitted to GenBank under the BioProject PRJNA546528. Genotypes used in estimating selection are available in Supplementary Information. Analytical input files and scripts for previously unpublished models in *dadi* are available through: <https://github.com/edgarwly>.

896 **Author Contributions**

897 DAF conceived and supervised the project. OGO and ASTP collected the samples and prepared  
898 them for sequencing. DAF measured leaf morphology. ELYW analysed the data with help from  
899 BN. ELYW wrote the draft of the manuscript, and all authors contributed to revisions.

900 **Tables and Figures**

901 **Table 1.** Recent studies estimating selection in hybrid zones using the approach of Barton & Gale (1993) using, ranked from highest to  
902 lowest estimates of selection strength.

Common name	Species	No. of loci	Selection estimates (CI)	Reference
<u>Selection estimated using <math>s = 8\sigma^2/w^2</math> (where <math>\sigma</math> = dispersal rate and <math>w</math> = cline width):</u>				
Salamander	<i>Ensatina eschscholtzii</i>	9	0.46 - 0.75 (NA)	Alexandrino et al., 2005
Rainforest skink	<i>Carlia rubrigularis</i> (N & S lineages)	9	0.50 – 0.70 (NA) 0.22 – 0.49 (NA)	Phillips et al., 2004
Rainforest lizard	<i>Lampropholis coggeri</i> (C & S lineages)	11	0.403 (0.106 – 0.653)	Singhal & Moritz, 2012
Swainson's thrush	<i>Catharus ustulatus ustulatus</i> & <i>C. u. swainsoni</i>	3	0.19 – 0.40 (NA)	Delmore & Irwin, 2014
European rabbit	<i>Oryctolagus cuniculus cuniculus</i> & <i>O. c. algirus</i>	28	0.20 (0.05 – 0.64)	Carneiro et al., 2013
Morabine grasshopper	<i>Vandiemena viatica</i> (2 chromosomal races)	10	0.197 (0.058 – 0.405)	Kawakami, Butlin, Adams, Paull, & Cooper, 2009
Yellow-rumped warbler	<i>Dendroica coronata coronata</i> & <i>D. c. auduboni</i>	2	0.18 (0.08 – 0.28)	Brelsford & Irwin, 2009
Ragwort	<i>Senecio aethnensis</i> & <i>S. chrysanthemifolius</i>	13	0.02 – 0.11 (NA)	Brennan et al., 2009
Common shrew	<i>Sorex araneus</i> (2 chromosomal races)	9	0.001 – 0.110 (NA)	Polyakov, White, Jones, Borodin, & Searle, 2011
		3	0.0003 – 0.003 (NA)	
House mouse	<i>Mus musculus musculus</i> & <i>M. m. domestica</i>	7	0.028 – 0.049 (NA)	Macholn et al., 2007
Red-backed fairy-wren	<i>Malurus melanocephalus melanocephalus</i> & <i>M. m. cruentatus</i>	102	0.007 (0.002 – 0.03)	Baldassarre, White, Karubian, & Webster, 2014
<u>Selection estimated using <math>s = 4\sigma^2/w^2</math>:</u>				
Crested Newt	<i>Triturus anatalicus</i> & <i>T. ivanbureschi</i>	49	0.11 (0.004 – 0.019)	Wielstra et al., 2017
Italian/ House sparrow	<i>Passer italiae</i> & <i>P. domesticus</i>	4	0.062 (0.038 – 0.109)	Bailey, Tesaker, Trier, & Sætre, 2015
Common/ Spined toad	<i>Bufo budo</i> & <i>B. spinosus</i>	32	0.0017 (0.0001 – 0.004)	van Riemsdijk et al. 2019
<u>Selection estimated using <math>s = 3\sigma^2/w^2</math>:</u>				
Stickleback	<i>Gasterostens aculeatus</i> (stream & anadromous ecotype)	7	0.097 (NA)	Vines et al., 2016
Marine gastropod	<i>Littorina saxatilis</i> (crab & wave ecotype)	57	0.06 (0.005 – 0.32)	Hollander, Galindo, & Butlin, 2015
		69	0.008 (NA)	

903

904 **Table 2.** Distribution of molecular variation at the individual, population and species/hybrid  
 905 group levels (AMOVA). Only individuals used in demographic modelling were included.

	df	Sum of squares	Variance component	% of variation
Among species/hybrid groups	3	25475.50	239.74	37.06
Among populations	8	5270.24	25.66	3.97
Among individuals	119	45403.84	381.55	58.98
Total	130	76149.586	646.949	100

906 **Table 3.** The likelihood of each demographic model investigated in *dadi* for each species/species or species/hybrid pair, results of likelihood  
907 ratio test (LRT) for certain nested models, Akaike information criterion (AIC) scores,  $\Delta$ AIC scores (relative to best model), and the relative  
908 likelihood of each model compared with the best model, and their respective parameter estimate.

Pops	Model	No. of free param.	<i>dadi</i>					LRT		N <sub>1</sub>	N <sub>2</sub>	T	s	P
			log- likelihood	theta	AIC			2ΔLL	P-value					
					AIC	ΔAIC	Rel.likelihood							
C/A	eSplitExpMig	6	-197.31	392.91	406.62	7.54	0.0230			0.20	0.25	0.83	0.29	
	SplitExpMig	5	-198.70	540.87	407.39	8.32	0.0156			0.15	0.22	0.99		
	split_mig	4	-198.61	616.79	405.23	6.15	0.0462			0.13	0.20	1.10		
	split	3	-264.45	367.97	534.91	135.83	0.0000	131.68*	1.76E-30	0.28	0.28	0.23		
	IMpre	8	-196.96	216.71	409.92	10.85	0.0044			0.38	0.42	4.05	0.34	
	IM	6	-197.52	476.12	407.03	7.96	0.0187	1.11	0.57	0.15	0.16	0.66	0.33	
	IM1	5	-223.52	404.69	457.04	57.96	0.0000	52.00*	5.55E-13	0.16	0.20	0.35	0.65	
	IM2	5	-230.70	358.62	471.40	72.33	0.0000	66.37*	3.74E-16	0.19	0.35	0.40	0.21	
	<b>IM2M</b>	<b>7</b>	<b>-192.54</b>	<b>433.13</b>	<b>399.07</b>	<b>0</b>	<b>1</b>			<b>0.20(0.18-0.22)</b>	<b>0.21(0.17-0.25)</b>	<b>0.70(0.45-0.95)</b>	<b>0.14(0.12-0.17)</b>	<b>0.42(0.33-0.52)</b>
	IM2M_1	5	-197.56	411.37	405.13	6.05	0.0485	10.05*	0.0066	0.18	0.25	0.98	0.35	
	SC	6	-212.66	182.06	437.32	38.25	0.0000			0.41	0.52			
	eSC	7	-196.45	384.47	406.89	7.82	0.0201			0.18	0.13		0.30	
	<b>SC_IM2M</b>	<b>8</b>	<b>-191.57</b>	<b>372.96</b>	<b>399.14</b>	<b>0.07</b>	<b>0.9666</b>			<b>0.22(0.22-0.23)</b>	<b>0.10(0.10-0.10)</b>		<b>0.23(0.22-0.24)</b>	<b>0.26(0.20-0.32)</b>
	IM2M_AL_SC	11	-194.14	290.02	410.27	11.20	0.0037			0.25	0.23		0.27	0.23
C/LH	IM	6	-246.61	293.92						0.41	0.82	4.55	0.44	
	IM2M	7	-253.23	297.13						0.27	0.88	3.52	0.31	0.13
C/HH	IM	6	-194.68	382.58						0.26	0.23	0.50	0.18	
	IM2M	7	-198.61	366.80						0.26	0.27	0.42	0.07	0.43
A/LH	IM	6	-234.40	506.69						0.25	0.24	2.19	0.58	
	IM2M	7	-222.65	404.34						0.31	0.24	0.66	0.26	0.03
A/HH	IM	6	-173.99	333.27						0.44	0.37	1.02	0.42	
	IM2M	7	-165.41	355.74						0.39	0.33	0.37	0.10	0.11
HH/LH	IM	6	-219.19	397.19						0.30	0.33	1.43	0.31	
	IM2M	7	-218.61	358.97						0.32	0.34	0.71	0.41	0.64

909 **Table 3.** (continued)

Pops	Model	M <sub>A</sub>	M <sub>B</sub>	M <sub>C</sub>	M <sub>D</sub>	M <sub>12</sub>	M <sub>21</sub>	M <sub>S</sub>	M <sub>E</sub>	M	T <sub>a</sub>	T <sub>s</sub>	T <sub>m</sub>	T <sub>pre</sub>	N <sub>pre</sub>
C/A	eSplitExpMig							0.41	0.75						
	SplitExpMig							0.93	1.01						
	split_mig									1.14					
	split									0†					
	IMpre					0.31	0.53							0.22	4.31
	IM					0.76	1.24								
	IM1					0†	1.03								
	IM2					0.62	0†								
	<b>IM2M</b>	<b>0.31(0.29-0.33)</b>	<b>1.36(0.12-0.15)</b>												
	IM2M_1	0.74	0†												
	SC					0.42	0.63				3.04	0.83			
	eSC					0.62	0.77				0.31	0.64			
	<b>SC_IM2M</b>	<b>2.23(0.22-0.23)</b>	<b>0.45(0.42-0.48)</b>								<b>0.38(0.37-0.39)</b>	<b>0.46(0.44-0.48)</b>			
	IM2M_AL_SC	1.93	0.45	2.34	0.16						0.18	3.86	4.25		
C/LH	IM					1.73	3.74								
	IM2M	1.47	3.31												
C/HH	IM					0.77	2.33								
	IM2M	0.86	1.97												
A/LH	IM					1.28	2.01								
	IM2M	0.98	3.41												
A/HH	IM					1.73	4.09								
	IM2M	0.55	4.70												
HH/LH	IM					3.72	3.04								
	IM2M	3.61	2.26												

Remarks: under the 'Pops' column: C = *S. chrysanthemifolius*; LH = low-elevation hybrids; HH = high-elevation hybrids; A = *S. aethnensis*; the two best-fitting models are in bold and italic; in all cases, likelihood ratio tests are for the comparison with the model immediately above except for IM2, which is for comparison with IM; Under 'LRT', \* indicates significant value; † indicates fixed value of parameters. Values in brackets for the models *IM2M* and *SC\_IM2M* are confidence intervals obtained from bootstrapping. Refer to Figure S2 for definitions of parameters.



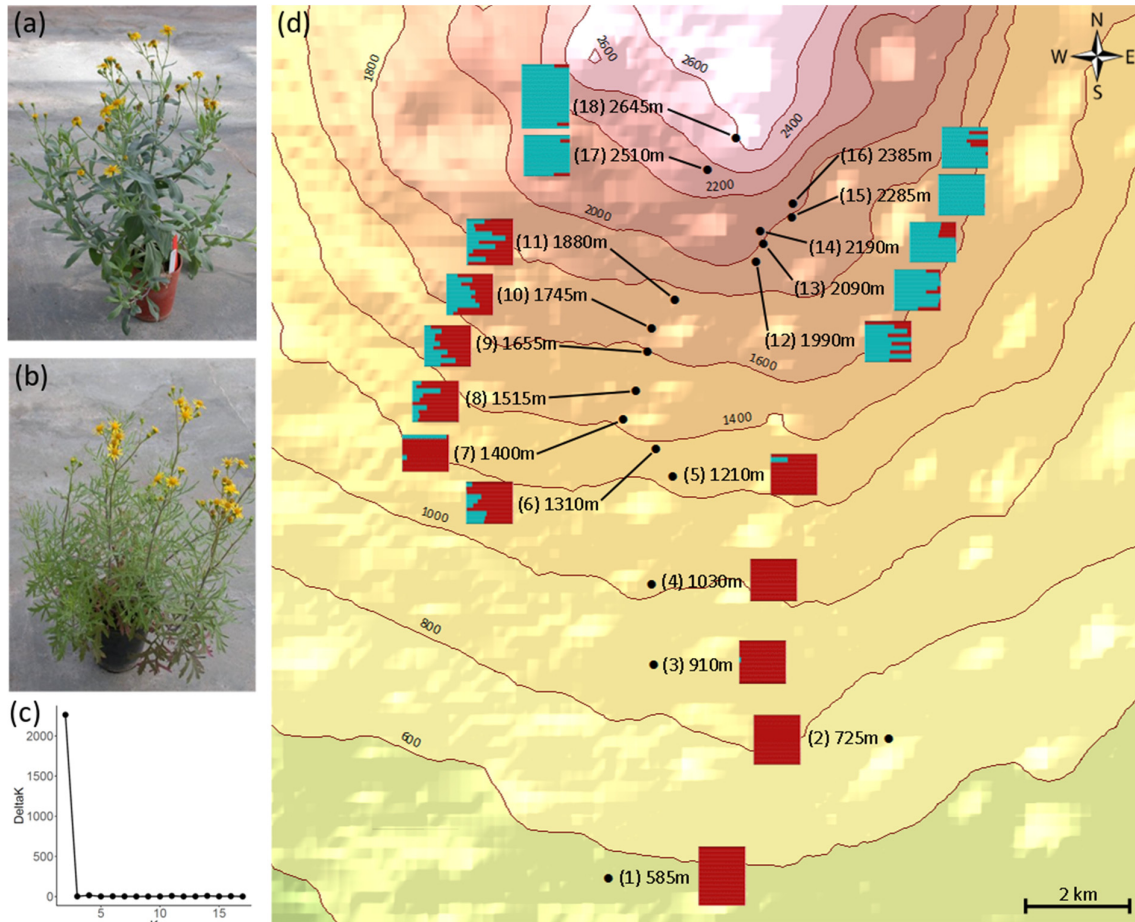
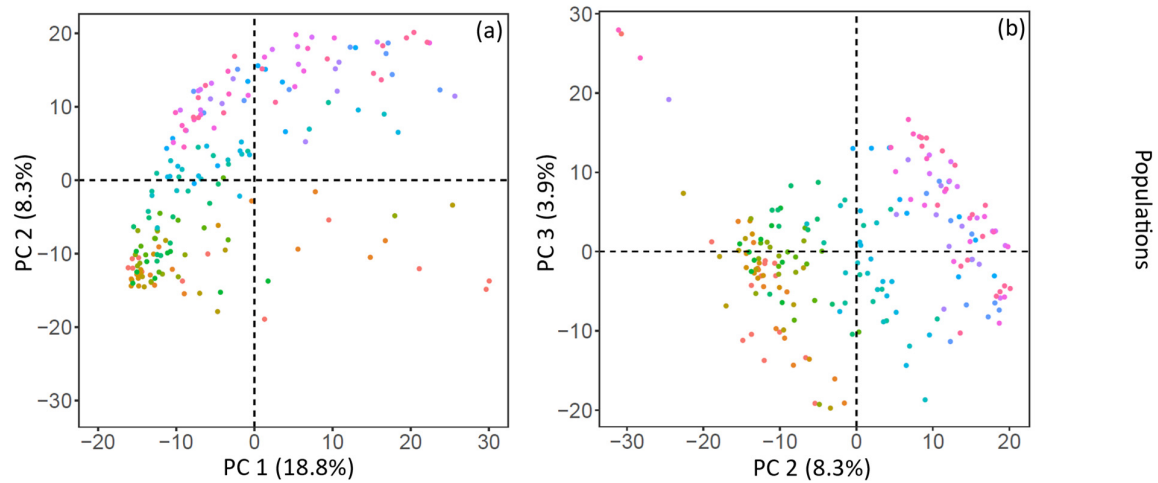
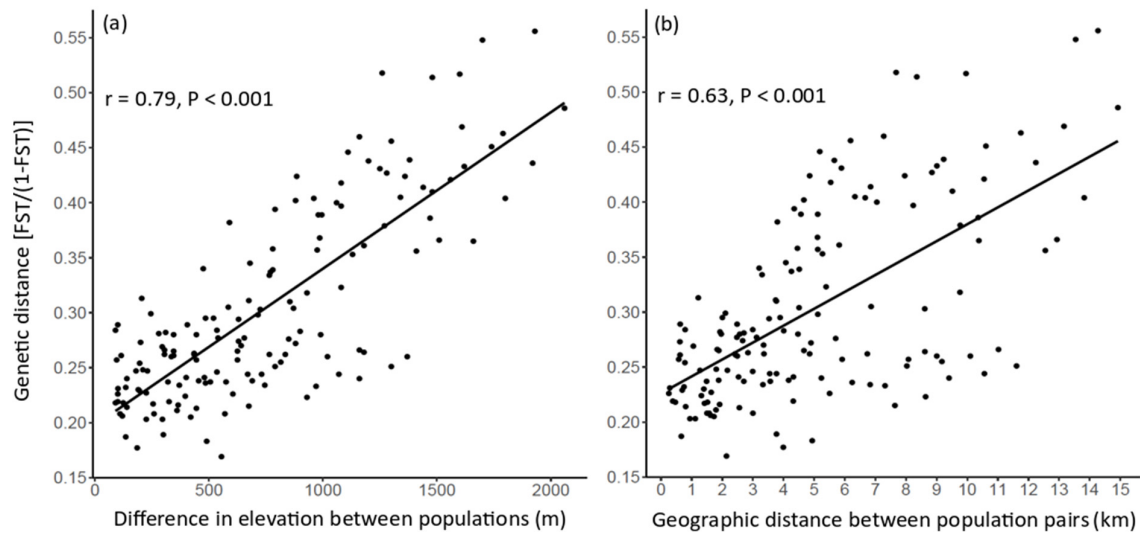


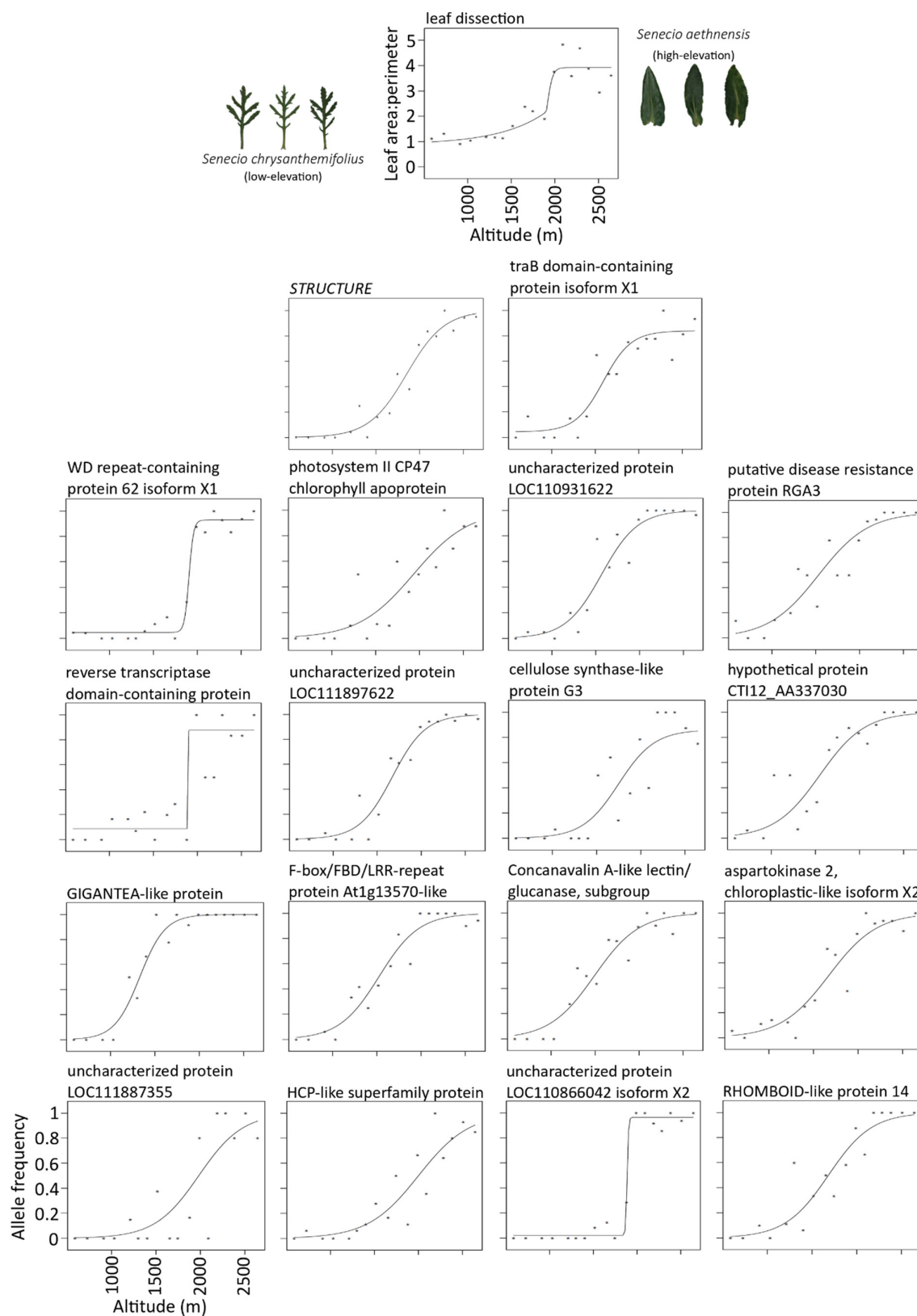
**Figure 1.** Distribution of sampled populations on Mount Etna and their genetic structure. (a) Photo of the high-elevation species *Senecio aethnensis* (obtained from senecioDB, undated). (b) Photo of the low-elevation species *Senecio chrysanthemifolius* (obtained from senecioDB, undated). (c)  $\Delta K$  plot showing optimal  $K = 2$ . (d) Contour map showing the southern side of Mount Etna using Google Earth Pro (Google) and ArcGIS (ESRI). Each black dot represents a sampled site. Numbers in brackets represent population numbers and numbers next to them are elevations where they were sampled. Coloured rectangular plots next to each site represent its corresponding section in the *STRUCTURE* plot (using 1,769 nextRAD markers with less than 50% missing data and  $K = 2$ ).



919 **Figure 2.** Plots from principle component analysis using 1,769 SNPs with less than 50% missing  
 920 data. (a) PC 1 and 2. (b) PC 2 and 3. Points beyond -30 in both axes in (a) were not shown to  
 921 allow comparable axis scales with (b). Full graph available in Figure S8.



922 **Figure 3.** Mantel test for genetic distance,  $F_{ST}/(1-F_{ST})$  and (a) difference in elevation between  
 923 population pairs; (b) geographic distance between population pairs.



924 **Figure 4.** Clines for leaf dissection, *STRUCTURE*, and allele frequencies at 17 outlier SNPs

925 located in genes with functional annotation available (see Table S3 for details). Each asterisk  
926 in the plots represents mean trait value, ancestry score, or allele frequency for each  
927 population. Examples of leaf shape of each species are shown next to the leaf dissection cline.

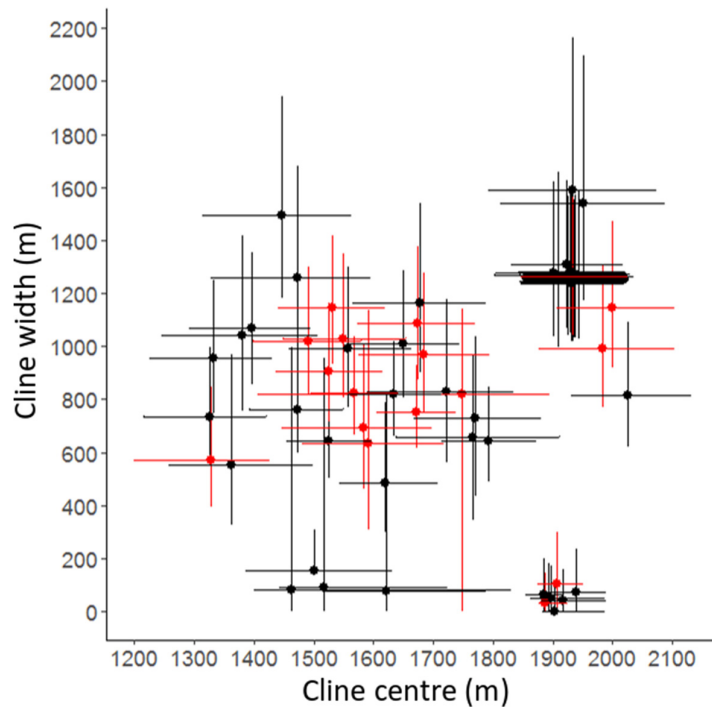


**Figure 5.** Variable cline coincidence and concordance of outlier clines. Maximum likelihood-estimated cline widths and cline centres of each outlier SNP are plotted as dots, while support limits are plotted as lines extending from the dots. Black and red data points represent non-outlier and outlier SNPs respectively. Refer to Table S4 for test results.

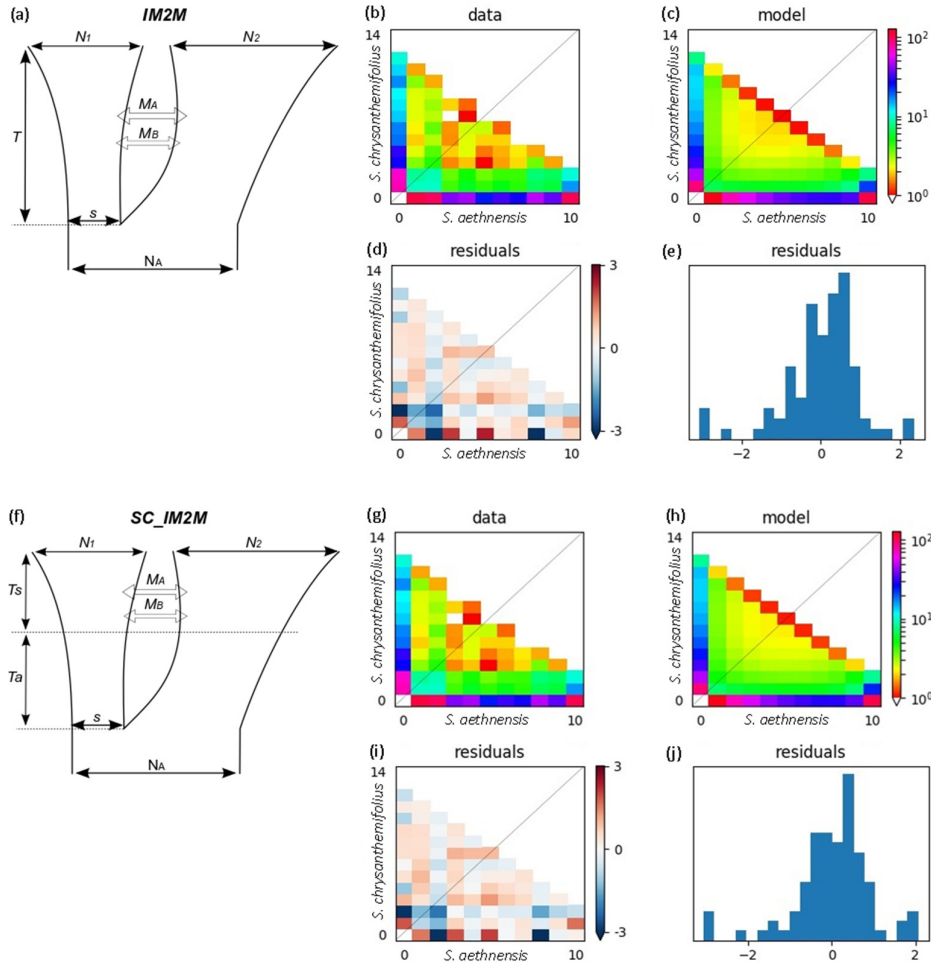


**Figure 6.** The fit of the two best demographic model (*IM2M* and *SC\_IM2M*) to site frequency spectrum data for *S. aethnensis* and *S. chrysanthemifolius*. (a) and (f) Schematic representation of the two best demographic model. Each model has four corresponding figures each: (b)-(e) for *IM2M* and (g)-(j) for *SC\_IM2M*. (b) and (g) Observed two-dimensional site-frequency-spectrum (2D-SFS). (c) and (h) 2D-SFS expected under the respective model. (d)-(e), (i)-(j) Residuals between the observed and the expected site-frequency-spectra.